| Title | Enzymatic glucose biosensor based on ZnO nanorod array grown by hydrothermal decomposition |
| --- | --- |
| Author(s) | Wei, A.; Sun, Xiaowei; Wang, J. X.; Lei, Y.; Cai, X. P.; Li, Chang Ming; Dong, Zhili; Huang, W. |
| Citation | Wei, A., Sun, X., Wang, J. X., Lei, Y., Cai, X. P., Li, C. M., et al. (2006). Enzymatic glucose biosensor based on ZnO nanorod array grown by hydrothermal decomposition. Applied Physics Letters, 89. |
| Date | 2006 |
| URL | http://hdl.handle.net/10220/6883 |
| Rights | |

# Enzymatic glucose biosensor based on ZnO nanorod array grown by hydrothermal decomposition

A. Wei

*Department of Physics, Fudan University, Shanghai 200433, China and School of Electrical & Electronic Engineering, Nanyang Technological University, Nanyang Avenue, Singapore 639798, Singapore*

X. W. Sun[a)] and J. X. Wang

*School of Electrical & Electronic Engineering, Nanyang Technological University, Nanyang Avenue, Singapore 639798, Singapore and Institute of Microelectronics, 11 Science Park Road, Science Park II, Singapore 117685, Singapore*

Y. Lei, X. P. Cai, and C. M. Li

*School of Chemical and Biomedical Engineering, Nanyang Technological University, Nanyang Avenue, Singapore 639798, Singapore*

Z. L. Dong

*School of Materials Science and Engineering, Nanyang Technological University, Nanyang Avenue, Singapore 639798, Singapore*

W. Huang

*Institute of Advanced Materials, Nanjing University of Posts and Telecommunications, Nanjing 210003, China*

We report herein a glucose biosensor based on glucose oxidase (GOx) immobilized on ZnO nanorod array grown by hydrothermal decomposition. In a phosphate buffer solution with a *p*H value of 7.4, negatively charged GOx was immobilized on positively charged ZnO nanorods through electrostatic interaction. At an applied potential of +0.8 V versus Ag/AgCl reference electrode, ZnO nanorods based biosensor presented a high and reproducible sensitivity of 23.1 $\mu$A cm$^{-2}$ mM$^{-1}$ with a response time of less than 5 s. The biosensor shows a linear range from 0.01 to 3.45 mM and an experiment limit of detection of 0.01 mM. An apparent Michaelis-Menten constant of 2.9 mM shows a high affinity between glucose and GOx immobilized on ZnO nanorods. © *2006 American Institute of Physics*. [DOI: 10.1063/1.2356307]

Biosensors including glucose biosensors are becoming increasingly important due to their applications in biological and chemical analyses, clinical detection, and environmental monitoring.[1,2] Among the numerous reports in glucose biosensors, the immobilization of enzymes on electrodes is generally the first step in fabrication, and thus, has attracted significant efforts, because enzymes are highly selective and quickly responsive to specific substrates. The immobilization of glucose oxidase (GOx), a widely used analytical enzyme for glucose detection, has been realized by various methods, such as physical adsorption,[3] cross-linking,[4] self-assembly,[5] incorporation in carbon paste,[6] polymers,[7] and sol gels,[8] etc.

On the other hand, nanomaterials have unique advantages in immobilizing enzyme and could retain its bioactivity due to the desirable microenviroment and the direct electron transfer between the enzyme's active sites and the electrode.[9,10] Biosensors, in particular, glucose biosensors, making use of titania sol-gel membrane,[8] carbon nanotubes,[11] Au nanoparticles,[12] TiO$_2$ nanoporous film,[13] and ZrO$_2$/chitosan composite film[14] to immobilize enzyme, have been reported. Recently, zinc oxide and its one-dimensional (1D) nanostructures have been investigated intensively due to their potential applications in optoelectronics.[15,16] ZnO nanodevices, such as transistors,[17] lasers,[18,19] and field emitters,[20] have been studied extensively. On the other hand, ZnO nanostructures have unique advantages including high

specific surface area, nontoxicity, chemical stability, electrochemical activity, and high electron communication features (ZnO is a widely used transparent conductor).[15] However, application of 1D ZnO nanostructures in biosensors is rare.[10] As ZnO has a high isoelectric point (IEP) of about 9.5, it is suitable for adsorption of low IEP proteins or enzyme such as GOx (IEP ~4.2). At the physiological *p*H value of 7.4, positively charged ZnO nanorods matrix not only provides a friendly microenvironment for immobilizing negatively charged GOx and retain its bioactivity, but also promotes electron transfer between GOx and the electrode to a large extent.[10] We have reported recently a glucose biosensor made of ZnO nanocomb grown by vapor-phase transport.[21] In this letter, we shall report a glucose biosensor based on GOx-modified ZnO nanorod array fabricated by hydrothermal decomposition.

ZnO nanorods were directly grown on a standard gold electrode commonly used in electrochemistry with an area of 0.02 cm$^2$ by hydrothermal decomposition. The reaction solution was prepared by mixing proper quantity of ammonia (25%) and 0.1*M* zinc chloride solution in a bottle with autoclavable screw cap. The gold electrode was horizontally immersed in the reaction solution. A layer of product was deposited on the gold electrode after the sealed bottle was heated at 95 °C for 90 min in an oven. Then, the sample was thoroughly washed with de-ionized water and dried in air. For immobilization of GOx (40 units/mg) on the as-grown ZnO nanorods, a 4 $\mu$l GOx solution with concentration of 30 mg/mL prepared in 0.01*M* phosphate buffer solution

---

a)Author to whom correspondence should be addressed; electronic mail: exwsun@ntu.edu.sg
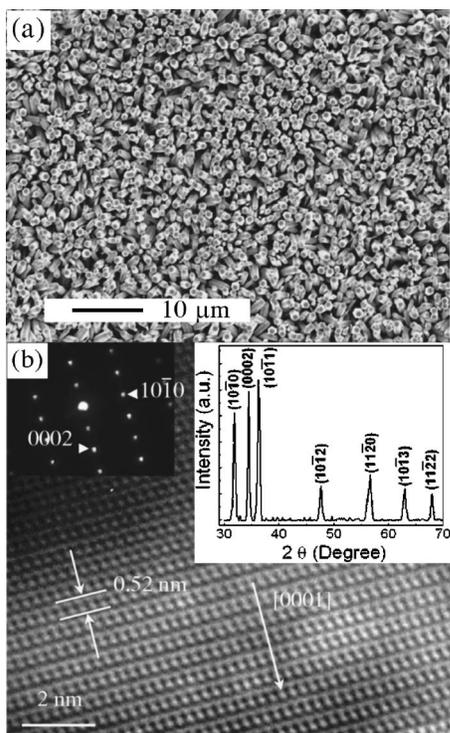
FIG. 1. (a) SEM image of the as-grown ZnO nanorod array on gold-coated glass substrate. (b) HRTEM image of a ZnO nanorod. The upper-left inset shows the corresponding SAED pattern. The zone axis is $[\bar{1}2\bar{1}0]$. The upper-right inset shows the XRD pattern of the ZnO nanorod array.



FIG. 2. Cyclic voltammograms of GOx/ZnO nanorods/Au electrode in the absence (a) and presence (b) of 5 mM glucose in 0.01$M$ PBS buffer ($p$H 7.4). Scan rate: 50 mV/s.

(PBS) ($p$H 7.4) was dropped on the ZnO film and kept at 4 °C overnight followed by an extensively washing step to remove the unimmobilized GOx. Finally, the electrode is ready for use.

A three electrode system consisting of a gold electrode with as-grown ZnO nanorods as working electrode, a platinum electrode as auxiliary electrode, and an Ag/AgCl reference electrode was employed for electrochemical experiments, which were carried out in a glass bottle containing 30 ml of 0.01$M$ PBS ($p$H 7.4). Cyclic voltammetric experiments were performed in an unstirred 0.01$M$ PBS buffer ($p$H 7.4). Amperometric measurements were carried out in a stirred solution (a magnetic stirring provided sufficient convective transport) with an applied potential of 0.8 V (versus Ag/AgCl), and the background current was allowed to decay to a steady-state before test. All the electrochemical experiments were carried out at room temperature. Scanning electron microscopy (SEM) was employed to examine the morphology of the hydrothermal product. The crystal structure of the sample was characterized by x-ray diffraction (XRD) using Cu $K\alpha$ radiation. The transmission electron microscope (TEM) was employed to observe the high resolution TEM (HRTEM) images and the selected area electron diffraction (SAED) pattern.

Figure 1(a) shows a typical SEM image of the as-grown product grown by hydrothermal decomposition. It can be seen that the nanostructure presents a rodlike shape with a hexagonal cross section, a typical morphology of wurtzite ZnO. It is also noted that the nanorods are primarily aligned along the perpendicular direction of the substrate. The nanorods are uniform in size with a diameter of about 300 nm and a length of 4 $\mu$m. The size uniformity is a unique feature of hydrothermally grown nanostructures compared to vapor phase transport method. Figure 1(b) shows a TEM image of
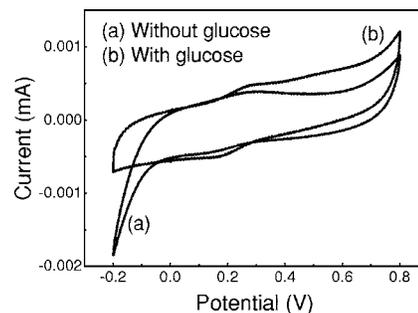
the ZnO nanorods. The lattice fringes in the HRTEM image with the $d$ spacing of 0.52 nm match the interspacing of (0001) planes of the wurtzite ZnO. These results demonstrate that the ZnO nanorods grew along [0001] direction. Consistent with the XRD pattern, the clear lattice image and SAED pattern indicate good crystalline quality of the ZnO nanorods. No dislocations or stacking faults are observed in the area examined. A representative XRD spectrum is shown in the upper-right inset of Fig. 1(b). As indexed in the pattern, all diffraction peaks match the wurtzite ZnO structure with the lattice constants of $a=3.250$ Å and $c=5.207$ Å. It is worth mentioning that there is some recess on the top of the nanorods, which can be seen from the SEM image and the XRD pattern.

It is known that ZnO has a high IEP of 9.5. In contrast, the IEP of GOx is about 4.2. Under our working condition ($p$H 7.4), the surface of ZnO nanorods is positively changed whereas GOx is negatively charged. Thus, immobilization of GOx on ZnO nanorods is highly favored through the electrostatic interaction. The cyclic voltammograms of the glucose biosensor in a 0.01$M$ PBS ($p$H 7.4) with or without glucose are shown in Fig. 2. Compared to the background observed in the absence of glucose for GOx/ZnO nanorods/Au electrode, the cyclic voltammogram changed dramatically with addition of 5 mM glucose. An obvious increase of oxidation current starting from about 0.2 V was observed.

Figure 3(a) displays amperometric response of the glucose biosensor for successive additions of glucose with 0.01, 0.03, 0.05, 0.1, 0.5, and 1 mM/step in 0.01$M$ PBS buffer ($p$H 7.4) at an applied potential of 0.8 V (versus Ag/AgCl) under stirring. The biosensor exhibit a rapid and sensitive response to the addition of glucose. As shown in Fig. 3, the curve shows a visible increase with the addition of 0.01 mM glucose relevant to the background current, which is attributed to good catalytic behavior of GOx/ZnO nanorods. The sensor achieves 95% of steady-state current in less than 5 s indicating a fast electron exchange between GOx and ZnO nanorods. The calibration curve of the sensor is shown in Fig. 3(b). The plot shows a linear range from 0.01 to 3.45 mM with a correction coefficient $R=0.9995$ and a high sensitivity (slope) of 23.1 $\mu$A cm$^{-2}$ mM$^{-1}$. The limit of detection (LOD) of glucose is 0.01 mM. According to the Lineweaver-Burk equation, the apparent Michaelis-Menten constant $K_M^{\mathrm{app}}$, a reflection of the enzymatic affinity, is calculated to be 2.9 mM (as shown in Fig. 3).[8] The high affinity of GOx to glucose can be attributed to ZnO nanorods due to their biocompatibility, large surface area, and high electron communication capability.
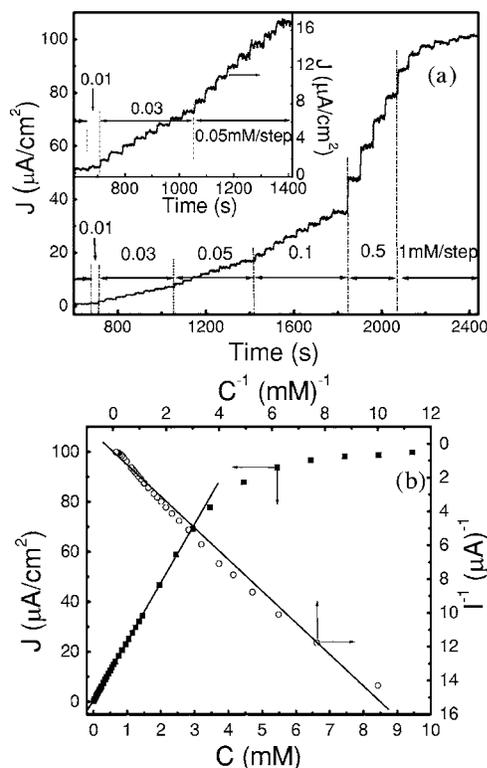
FIG. 3. (a) Amperometric responses of GOx/ZnO nanorods/Au electrodes with successive addition of glucose to the 0.01*M* *p*H 7.4 PBS buffer under stirring. The applied potential was +0.8 V (vs Ag/AgCl reference). The inset shows the enlarged response for low concentration (0.01, 0.03, and 0.05 mM) of glucose additions. (b) Calibration curves for glucose using GOx/ZnO nanorods/Au electrode (solid squares) and the Lineweaver-Burk plot (open circles). The straight line is a linear fit to the plot.

For comparison, Table I tabulates the key parameters of the glucose biosensors reported in this work and those previous papers making use of various nanomaterials as the working electrode. From Table I, we can see that the ZnO nanorods biosensor show high sensitivity (only lower than that of carbon nanotubes) and small $K_M^{app}$, which should be attributed to (1) high GOx loading owing to the large specific surface area of ZnO nanorods and the high affinity of GOx to glucose and (2) direct and fast electron path from ZnO na-

norods to the gold electrode. Meanwhile, the limit of detection and response time of ZnO nanorods are also among the best. Our results demonstrate that ZnO nanorod is an attractive material for electroanalytical measurements, and has great potential in the sensor construction due to their biomimetic and high electron communication features. The glucose biosensor retained about 65% of its original sensitivity after one week storage in 0.01*M* PBS (*p*H 7.4) at 4 °C. With Nafion modification, the biosensor did not show significant decrease in sensitivity ($<5\%$) under the same storage condition for 1 week.

In conclusion, our glucose biosensor based on hydrothermally grown ZnO nanorods and GOx exhibits a low LOD of 0.01 mM, a high and reproducible sensitivity of 23.1 $\mu$A cm$^{-2}$ mM$^{-1}$ with a response time of less than 5 s, a linear range from 0.01 to 3.45 mM, and an apparent $K_M^{app}$ of 2.9 mM. These parameters demonstrate that ZnO nanorods can provide a favorable microenvironment for the GOx immobilization and stabilize its biological activity to a large extent due to high specific surface area, biomimetic, and high electron communication features. In fact, ZnO nanorods can provide an efficient electronconducting tunnel and facilitate the electron transfer.[21] The hydrothermal deposition method provides a cheap yet efficient method to grow ZnO nanostructures for biosensor application. It would probably provide an economic way to meet the industrial requirements of low-cost processing technique for large-scale production.

TABLE I. Key performance parameters of glucose electrochemical biosensors making use of various GOx-modified nanomaterials as the working electrodes.

| Electrode material | Applied potential (V) | $K_M^{app}$ (mM) | Sensitivity ($\mu$A cm$^{-2}$ mM$^{-1}$) | LOD ($\mu$M) | Response time (s) | Ref. |
|---|---|---|---|---|---|---|
| Titania sol-gel membrane | 0.3 | 6.34 | 7.2 | 70 | <6 | 8 |
| Carbon nanotubes | 0.55 | ⋯ | 30.14 | 0.5 | <3 | 11 |
| Au nanoparticles | 0.3 | 4.3 | 8.8 | 8.2 | <8 | 12 |
| TiO$_2$ nanoporous film | 0.7 | 6.08 | 4.58 | ⋯ | <30 | 13 |
| ZrO$_2$/chitosan film | 0.5 | 3.14 | 0.028 | 10 | <10 | 14 |
| ZnO nanocombs | 0.8 | 2.19 | 15.33 | 20 (measured) | <10 | 21 |
| ZnO nanorods | 0.8 | 2.9 | 23.1 | 10 (measured) | <5 | This work |

[1]N. A. Rakow and K. S. Suslick, Nature (London) **406**, 710 (2000).
[2]R. W. Keay and C. J. McNeil, Biosens. Bioelectron. **13**, 963 (1998).
[3]F. Battaglini, P. N. Bartlett, and J. H. Wang, Anal. Chem. **72**, 502 (2000).
[4]J. J. Burmeister and G. A. Gerhardt, Anal. Chem. **73**, 1037 (2001).
[5]A. S. N. Murthy and J. Sharma, Anal. Chim. Acta **363**, 215 (1998).
[6]J. Kulys, L. Tetianec, and P. Schneider, Biosens. Bioelectron. **16**, 319 (2001).
[7]F. Palmisano, R. Rizzi, D. Entonze, and P. G. Zambonin, Biosens. Bioelectron. **15**, 531 (2000).
[8]J. H. Yu, S. Q. Liu, and H. X. Ju, Biosens. Bioelectron. **19**, 401 (2003).
[9]J. B. Jia, B. Q. Wang, A. G. Wu, G. G. Cheng, Z. Li, and S. J. Dong, Anal. Chem. **74**, 2217 (2002).
[10]F. F. Zhang, X. L. Wang, S. Y. Ai, Z. D. Sun, Q. Wan, Z. Q. Zhu, Y. Z. Xian, L. T. Jin, and K. Yamamoto, Anal. Chim. Acta **519**, 155 (2004).
[11]S. Hrapovic, Y. L. Liu, K. B. Male, and J. H. T. Luong, Anal. Chem. **76**, 1083 (2004).
[12]Y. H. Yang, H. F. Yang, M. H. Yang, Y. L. Liu, G. L. Shen, and R. Q. Yu, Anal. Chim. Acta **525**, 213 (2004).
[13]T. J. Chara, R. Rajagopalan, and A. Heller, Anal. Chem. **66**, 2451 (1994).
[14]K. Ogata, K. Koike, T. Tanite, T. Komuro, S. Sasa, M. Inoue, and M. Yano, Sens. Actuators B **100**, 209 (2004).
[15]X. W. Sun and H. S. Kwok, J. Appl. Phys. **86**, 408 (1999).
[16]C. X. Xu, X. W. Sun, C. Yuen, B. J. Chen, S. F. Yu, and Z. L. Dong, Appl. Phys. Lett. **86**, 011118 (2005).
[17]W. I. Park, J. S. Kim, G.-C. Yi, M. H. Bae, and H.-J. Lee, Appl. Phys. Lett. **85**, 5052 (2004).
[18]M. Huang, S. Mao, H. Feick, H. Yan, Y. Wu, H. Kind, E. Weber, R. Russo, and P. Yang, Science **292**, 1897 (2001).
[19]X. W. Sun, S. F. Yu, C. X. Xu, C. Yuen, B. J. Chen, and S. Li, Jpn. J. Appl. Phys., Part 2 **42**, L1229 (2003).
[20]C. X. Xu and X. W. Sun, Appl. Phys. Lett. **83**, 3806 (2003).
[21]J. X. Wang, X. W. Sun, A. Wei, Y. Lei, X. P. Cai, C. M. Li, and Z. L. Dong, Appl. Phys. Lett. **88**, 233106 (2006).